An integrated microfluidic processor for single nucleotide polymorphism-based DNA computing

William H. Grover and Richard A. Mathies*

Received 26th April 2005, Accepted 21st July 2005
First published as an Advance Article on the web 11th August 2005
DOI: 10.1039/b505840f

An integrated microfluidic processor is developed that performs molecular computations using single nucleotide polymorphisms (SNPs) as binary bits. A complete population of fluorescein-labeled DNA "answers" is synthesized containing three distinct polymorphic bases; the identity of each base (A or T) is used to encode the value of a binary bit (TRUE or FALSE). Computation and readout occur by hybridization to complementary capture DNA oligonucleotides bound to magnetic beads in the microfluidic device. Beads are loaded into sixteen capture chambers in the processor and suspended in place by an external magnetic field. Integrated microfluidic valves and pumps circulate the input DNA population through the bead suspensions. In this example, a program consisting of a series of capture/rinse/release steps is executed and the DNA molecules remaining at the end of the computation provide the solution to a three-variable, four-clause Boolean satisfiability problem. The improved capture kinetics, transfer efficiency, and single-base specificity enabled by microfluidics make our processor well-suited for performing larger-scale DNA computations.

Introduction

Ten years after the invention of the transistor, microfabrication methods were devised to efficiently pack transistors onto silicon chips, and the now-ubiquitous integrated circuit was born. In 1994 Adleman used DNA to perform the first molecular computation.[1] This and subsequent implementations of molecular computing would similarly benefit from the development of a *molecular integrated circuit*—a device to automate, miniaturize, and parallelize molecular computing operations. An integrated circuit for DNA computation was first described conceptually in 1999 as an array of microreactors with DNA oligonucleotides immobilized in the reactors for sequence-specific capture and redirection of input DNA, together with a microfluidic pumping mechanism for routing DNA solutions between the reactors.[2] In this hypothetical computer, input oligonucleotide populations encoding all possible answers to a given problem would be introduced into the device, a series of sequence-specific capture and release operations would separate oligonucleotides encoding incorrect answers from those encoding correct ones, and any input oligonucleotides remaining at the end of the computation would encode the correct solution or solutions to the problem. Execution of this vision was difficult in 1999 because the available microfluidic valve, pump, and capture technologies were chemically or physically unsuitable for use with DNA or were difficult to fabricate in the dense arrays required for the molecular computer.[3–8]

Significant progress has subsequently been made using beads trapped in microfluidic devices for sequence-specific capture of oligonucleotides in computational[9,10] and in analytical[11–16] applications. However, since typical structures lack active fluid control, only a single pass of an input DNA solution through the beads is possible, and the ability of these devices to successfully capture and route DNA is limited. In part to compensate for poor capture kinetics, many demonstrations of hybridization-based DNA computing have used long hybridization times and multiple-base capture sequences to represent single binary bits. The most complex DNA computation performed to date was solved using 300 base pair input DNA containing constant 15-base sequences for each of 20 binary bits.[17] The computation required 4 hours for each of 24 hybridization steps for a total runtime of 96 hours. Recent advances in DNA microarray technology clearly demonstrate that constant multi-base capture sequences and extensive hybridization times are not in principle required for reliable molecular recognition.[18]

Recently, we developed a novel pneumatic membrane valve and pump design that enables the fabrication of dense, large-scale arrays of actuators on glass microfluidic devices.[19] These valve technologies have thus far been instrumental in the development of integrated genetic analyzers for DNA sequencing and analysis,[20] pathogen and infectious disease detectors,[21] and amino acid analysis systems for space exploration.[22] Here we exploit this pneumatic membrane valve and pump technology to develop and demonstrate a microfluidic processor for performing DNA computations using single nucleotide polymorphisms (SNPs) as binary bits.

Our processor interrogates an 11-base long fluorescein-labeled input DNA population that includes three polymorphic bases for a total of eight unique sequences. These eight sequences represent all possible solutions to a three-bit computation, with the actual base at each polymorphism (A or T) representing a binary value (TRUE or FALSE) for the bit

Department of Chemistry, University of California, Berkeley, CA 94720, USA. E-mail: rich@zinc.cchem.berkeley.edu; Fax: +1 (510) 642-3599; Tel: +1 (510) 642-4192

This journal is © The Royal Society of Chemistry 2005

associated with the polymorphism. The processor shown in Fig. 1 includes an array of 16 capture chambers (A–P) containing magnetic beads derivatized with biotinylated capture oligonucleotides complementary to specific members of the input population. An integrated monolithic membrane diaphragm pump and 32 bus valves are used to circulate input oligonucleotides through the bead suspensions in selected capture chambers. Correct answers (perfectly-complementary oligonucleotides) are captured by hybridization, and incorrect answers are eliminated by rinsing the bead suspension. Oligonucleotides remaining after a series of capture/rinse/release steps represent correct solutions to the logical satisfiability problem encoded in the path followed by the oligonucleotides through the device. The enhanced capture and transfer efficiency provided by microfluidics makes possible this first demonstration of a hybridization-based DNA computation using SNPs to represent binary bits.

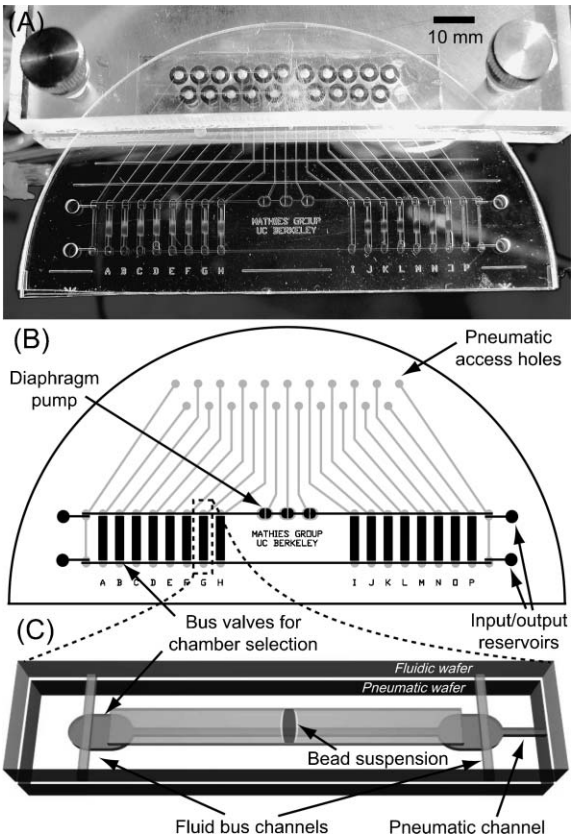

Fig. 1 Photograph (A) and mask design (B) of the microfluidic processor. Pneumatic (grey) and fluidic (black) features were etched into a single 10 cm diameter, 1.1 mm thick glass wafer that was subsequently split into the fluidic and pneumatic layers and bonded reversibly with the PDMS membrane. Twenty-one pneumatic access holes supply actuation vacuum (−60 kPa) and pressure (10 kPa) to the three pump valves, 32 bus valves, and four input/output valves. (C) Oblique view of a single capture chamber. When vacuum is applied to a pneumatic channel, the bus valves open as the PDMS membrane pulls away from the fluidic wafer and flow in the fluid bus is diverted through the capture chamber. Magnetic beads (12 μg per chamber) are held in place by rare earth magnets placed above and below the processor (not shown). Each chamber contains 1.1 μL of fluid; a typical active volume of the device while circulating (chambers A and O plus the volume contained in the fluidic loop and pump valves) is 5.8 μL.

Methods

Device fabrication

Device features (see Fig. 1) were etched into glass wafers using conventional photolithography and wet chemical etching.[23] Briefly, 1.1 mm thick, 100 mm diameter borosilicate glass wafers were coated with 200 nm of polysilicon using low-pressure chemical vapor deposition. The wafers were then spin-coated with positive photoresist, soft-baked, and patterned with the device design using a contact aligner and a chrome mask. After development and removal of irradiated photoresist, the exposed polysilicon regions were removed by etching in SF_6 plasma and the exposed regions of glass were etched isotropically in 49% HF to a depth of 100 μm. After stripping the remaining photoresist and polysilicon layers, the wafers were drilled with 1.1 mm diameter holes for pneumatic connections and 2.5 mm diameter holes for fluidic reservoirs. The wafers were then scored and broken, and the resulting fluidic and pneumatic layers were bonded using a 254 μm thick polydimethylsiloxane (PDMS) elastomer membrane.[19] Internal surfaces of the device were treated with a 5% bovine serum albumin solution before use to reduce adsorption of DNA.

Basis for computation

Computing with single DNA bases involves two related kinds of complementarity between the immobilized capture and fluorescent input DNA populations: base-wise (T and A) and bit-wise (TRUE and FALSE) complementarity. Arbitrarily, T represents TRUE and A represents FALSE for a given bit B_n in the biotinylated (Bio) capture population 5′-Bio-agB_0tcB_1caB_2gt-3′, and A represents TRUE and T represents FALSE for the same bit in the fluorescein-labeled (FAM) input population 5′-FAM-acB_2tgB_1gaB_0ct-3′. Capture by hybridization occurs only if the input and capture oligonucleotides are perfectly complementary, meaning that the bit values encoded in the input oligonucleotide satisfy all the logical requirements of the capture oligonucleotide. After a series of capture/rinse/release steps, input oligonucleotides remaining at the end of the series encode a solution that satisfies the conjunction (the Boolean AND) of the requirements at each individual step. If two or more different capture oligonucleotides are bound to beads in the same chamber, input oligonucleotides captured in the chamber encode a solution that satisfies the disjunction (the Boolean OR) of the requirements of the different capture oligonucleotides. Finally, capture oligonucleotides containing A at bit B_n capture only negated values of that bit (the Boolean NOT).[24] Using this method and our device, we set out to solve the 3-bit, 4-clause Boolean satisfiability problem

$$[\mathrm{NOT}(B_0)\ \mathrm{OR}\ B_2]\ \mathrm{AND}\ [B_0\ \mathrm{OR}\ B_1]\ \mathrm{AND}\ [\mathrm{NOT}(B_1)\ \mathrm{OR}\ \mathrm{NOT}(B_2)]\ \mathrm{AND}\ [\mathrm{NOT}(B_0)\ \mathrm{OR}\ B_1]$$

which is TRUE only if B_0 = FALSE, B_1 = TRUE, and B_2 = FALSE.

This journal is © The Royal Society of Chemistry 2005

Table 1 Sequences and computational roles of oligonucleotides

Synthesis (5′–3′)	Population members (5′–3′)		Computational role
Bio-agTtcWcaWgt (B_0 = TRUE)	Bio-agTtcTcaTgt Bio-agTtcAcaTgt	Bio-agTtcTcaAgt Bio-agTtcAcaAgt	captures B_0 = TRUE (FAM-acWtgWgaAct)
Bio-agWtcTcaWgt (B_1 = TRUE)	Bio-agTtcTcaTgt Bio-agAtcTcaTgt	Bio-agTtcTcaAgt Bio-agAtcTcaAgt	captures B_1 = TRUE (FAM-acWtgAgaWct)
Bio-agWtcWcaTgt (B_2 = TRUE)	Bio-agTtcTcaTgt Bio-agAtcTcaTgt	Bio-agTtcAcaTgt Bio-agAtcAcaTgt	captures B_2 = TRUE (FAM-acAtgWgaWct)
Bio-agAtcWcaWgt (B_0 = FALSE)	Bio-agAtcTcaTgt Bio-agAtcAcaTgt	Bio-agAtcTcaAgt Bio-agAtcAcaAgt	captures B_0 = FALSE (FAM-acWtgWgaTct)
Bio-agWtcAcaWgt (B_1 = FALSE)	Bio-agTtcAcaTgt Bio-agAtcAcaTgt	Bio-agTtcAcaAgt Bio-agAtcAcaAgt	captures B_1 = FALSE (FAM-acWtgTgaWct)
Bio-agWtcWcaAgt (B_2 = FALSE)	Bio-agTtcTcaAgt Bio-agAtcTcaAgt	Bio-agTtcAcaAgt Bio-agAtcAcaAgt	captures B_2 = FALSE (FAM-acTtgWgaWct)
FAM-tcWagWgtWca (all 8 possible values for B_2, B_1, B_0)	FAM-acTtgTgaTct FAM-acTtgAgaTct FAM-acAtgTgaTct FAM-acAtgAgaTct	FAM-acTtgTgaAct FAM-acTtgAgaAct FAM-acAtgTgaAct FAM-acAtgAgaAct	input population

[a] Polymorphic bases used for bit encoding are capitalized. W in a synthesis run indicates either T or A. Bio and FAM indicate 5′ biotin and fluorescein oligonucleotide modifications, respectively.

Capture and input DNA populations

Six synthesis runs of 11-base biotinylated oligonucleotides provided the populations of capture oligonucleotides used in the computation (5′-Bio-agTtcWcaWgt-3′, Bio-agWtcTcaWgt, Bio-agWtcWcaTgt, Bio-agAtcWcaWgt, Bio-agWtcAcaWgt, and Bio-agWtcWcaAgt; W indicates either A or T and polymorphic bases are capitalized). To prepare each of the bead-oligonucleotide conjugates, 5 nmol of biotinylated oligonucleotides (Integrated DNA Technologies, Coralville, IA) and 85 μg of 1.5 μm diameter streptavidin-coated magnetic beads (Bangs Laboratories, Fishers, IN) were incubated in 50 μL TTL buffer (100 mM Tris-HCl, 0.1% Tween 20, 1.0 M LiCl) at room temperature for 3 h. The derivatized beads were then rinsed in 0.15 N NaOH to eliminate nonspecifically-bound oligonucleotides, then rinsed twice in TT buffer (250 mM Tris-HCl, 0.1% Tween 20), and finally incubated in TTE buffer (250 mM Tris-HCl, 0.1% Tween 20, 20 mM EDTA) at 80 °C for 10 min to remove any remaining unstable linkages. A single 11-base synthesis run of the fluorescein-labeled 5′-FAM-acWtgWgaWct-3′ provided the input DNA population for the computation and two additional syntheses (FAM-acWtgAgaWct and FAM-acWtgTgaWct) yielded the populations used in the characterization studies. Oligonucleotide sequences and experimental conditions were chosen to maximize the difference between the calculated melting temperatures of the least-stable perfectly-matched duplex (T_m = 47.3 °C) and the most-stable single-base-mismatched duplex (T_m = 37.8 °C), ensuring that capture occurs only between perfectly-complementary oligonucleotides.[25] The sequences and computational roles of the oligonucleotides are summarized in Table 1.

Programming the integrated circuit

The integrated circuit is programmed by loading the desired combinations of beads labeled with capture oligonucleotides into the various chambers on the device. Two sets of bus valves are opened to select the target chamber on the right side of the device and the input/output reservoirs on the left side. A suspension of beads (5 μL of a 2.5 μg μL^{-1} solution) in hybridization buffer (700 mM NaCl, 10% formamide, 10 mM phosphate pH 7.2, 0.1% Tween-20) is pumped from the left input reservoir through the selected chamber on the right side of the device, where they are captured by magnets placed above and below the chamber (Fig. 2A). The process is reversed (right input reservoirs to left chamber) when filling chambers on the left side of the device. The trapped beads are then rinsed by pumping 10 μL of fresh hybridization buffer through the bead suspension, and the loading process is repeated for each bead chamber. Next, a single "load" chamber is filled with a 30 μM solution of the fluorescent input population in hybridization buffer (Fig. 2B). Input solution is loaded until the entire volume of the load chamber plus the fluidic loop and three open pump valves is filled with the solution. This volume (5.8 μL) sets the amount of input DNA going into the first step of the computation (170 pmol),

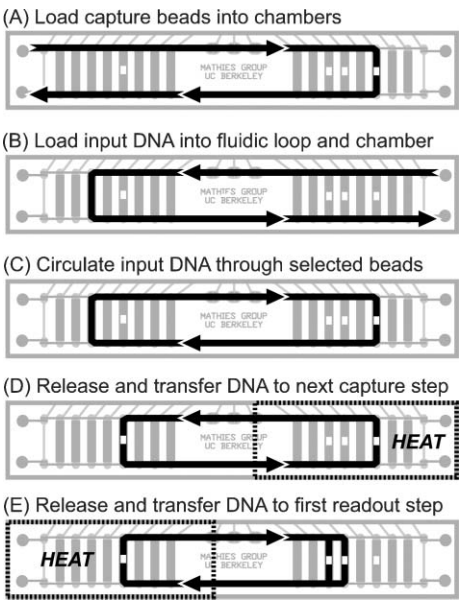

Fig. 2 Diagrams showing fluid flow during loading (A and B), capture (C), release and recapture (D) and readout (E) steps of the microfluidic processor.

which is nine times greater than the experimentally-determined capacity of the beads in the first capture chamber.

Performing the computation

In the first step of a computation, two sets of bus valves are opened to join the load chamber on the left side of the device and first capture chamber on the right side in the microfluidic circuit. With the magnet holding the bead suspension in place and the beads maintained at 25 °C, the 5.8 μL fluid contents of the device are pumped in a clockwise circuit through the load and capture chambers (Fig. 2C). The three pump valves are actuated according to a six-step, three second pumping pattern.[19] After 30 minutes of pumping (roughly 22 passes of the input oligonucleotide solution through the bead suspension), the load chamber is rinsed with buffer from the right input reservoir and the beads in the capture chamber are rinsed from the left input reservoir to eliminate incorrect (mismatched) input oligonucleotides. The beads are then collected against the edge of the chamber using the magnet and the uniform bed of beads is imaged using an inverted fluorescence microscope (Nikon) with excitation light from a mercury arc lamp passed through a 480 nm band-pass filter and reflected off a 505 nm long-pass dichroic beamsplitter through a 4× objective lens; the measured power at the objective was 17 mW. Fluorescence was collected back through the objective and passed through the dichroic and a 535 nm band-pass filter before impinging upon a CCD detector (QImaging, Burnaby, BC, Canada) for a 2 s exposure.

In the second step, the right-side bead chamber that captured input oligonucleotides in the *first* step is heated using an external heater to 50 °C (2 °C higher than the mean calculated T_m of the eight perfect complements) while maintaining the new *second* bead chamber on the left side of the device at 25 °C. Two sets of bus valves are opened to join the hot and cool chambers in the circuit, and the released input oligonucleotides are pumped counterclockwise between the old and new chambers (Fig. 2D). After 30 minutes of pumping, the chambers are again rinsed and imaged as described above. This back-and-forth process is then repeated for all computation chambers, with additional incorrect answers eliminated at each step.

To readout the result of a computation, input oligonucleotides captured in the last step of the computation are simultaneously transferred to *two* chambers, one containing beads capturing A (TRUE) for a given base/bit and the other capturing T (FALSE) (Fig. 2E). A special 45 min pumping cycle alternates flow between the two destination chambers every three seconds, and the beads are not rinsed after readout captures because no elimination of incorrect answers is occurring. The value of the bit is determined by comparing the relative fluorescence of the two chambers, and the overall solution to the problem is read by repeating the readout process for the other two bits.

Results

Bit fidelity and rinsing efficiency

To demonstrate the feasibility of using single-base polymorphisms to encode binary bits, chambers B and O were loaded with 12 μg of 5′-Bio-agWtcTcaWgt-3′ and 5′-Bio-agWtcAcaWgt-3′ beads, respectively. Two separate single-step captures were performed by filling the loop volume each time with an ~10× excess of 5′-FAM-acWtgAgaWct-3′ (5.8 μL of a 30 μM solution or 170 pmol) and using the on-chip diaphragm pump to circulate the solution through the beads for 30 min. Fig. 3 compares background-corrected

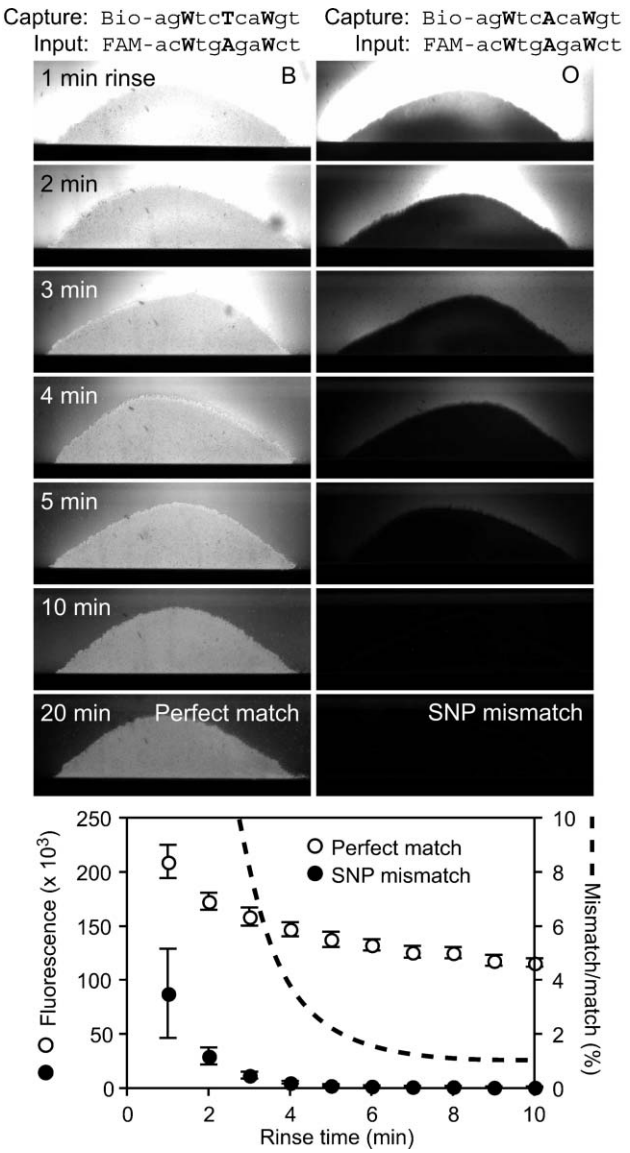

Fig. 3 Fluorescence images of capture beads in the bit fidelity and rinsing efficiency experiment. The sustained bead fluorescence with rinsing in chamber B confirms capture of the perfectly-complementary input population, while the rapid elimination of fluorescence with rinsing in chamber O verifies that single-base mismatches prevent capture. In the plot of fluorescence counts at various rinse times, the ratio of the single-base mismatch fluorescence (closed circles) to the perfectly-complementary fluorescence (open circles) provides an estimate of computational error associated with a single capture step (dashed line); an 8 min rinse reduces the error to 1.1%. Fluorescence count data was obtained by integrating over a region of constant area in each background-corrected image. Error bars indicate the standard deviation among individual pixel fluorescence values due to the spatial inhomogeneity within each bead bed.

This journal is © The Royal Society of Chemistry 2005

fluorescence images of beads in the two chambers at various times in the post-capture bead rinse. Every immobilized capture oligonucleotide in chamber B had a perfect complement in the fluorescent input population, and the resulting bead fluorescence started high and decreased slowly with rinsing. In contrast, every capture oligonucleotide in chamber O had at least a single base mismatch with every input oligonucleotide, and the observed fluorescence intensity started low and decreased quickly as mismatched input oligonucleotides were rinsed away. The ratio of mismatched to perfectly-complementary fluorescence (O/B) is a measurement of computational error introduced by incomplete capture of perfectly-matched input oligonucleotides and partial capture of mismatched input oligonucleotides. Rinsing the beads for three minutes reduced the error rate to 7.6%, and five additional minutes of rinsing further reduced the error rate to only 1.1%. Other results indicated that protocols utilizing more stringent hybridization buffers (less salt or more formamide) increased mismatch detection sensitivity at shorter rinse times, at the expense of decreased step-to-step transfer efficiency.

In a separate calibration experiment, after an eight minute rinse, the oligonucleotides captured in chamber B were heated and released into an on-chip loop of known volume. The fluorescence intensity of this solution was compared with intensities from a series of standards to determine that 18 pmol of the initial 170 pmol of input oligonucleotides were captured in chamber B. This result did not change significantly with the use of more concentrated input oligonucleotide solutions, indicating that in this and subsequent experiments the 18 pmol capacity of the *first* capture/rinse/release step determined the total amount of input DNA used in the device.

Serial capture/rinse/release efficiency

Fig. 4 presents the program used to determine the efficiency of serial capture and release on the microfluidic processor. Chambers A and O each contained 12 μg of Bio-agWtcTcaWgt beads; chamber P and the loop volume were loaded with an $\sim 10\times$ excess of FAM-acWtgAgaWct (5.8 μL of a 30 μM solution or 170 pmol). Since each oligonucleotide in the input population had an exact complement in the capture population, no elimination of mismatched input DNA occurred in this experiment. The input oligonucleotides were transferred back and forth eight times between chambers A and O, with 30 minutes per capture/rinse/release step and either three or eight minute rinse times after each capture. A measured pumping rate of 70 nL $s^{-1}$and a constant 5.8 μL loop volume indicate that during each 30 min capture/rinse/release step the contents of the loop were passed through the beads ~ 22 times. Fig. 4 shows fluorescent images of beads in chambers A and O after each of the eight steps. The more-stringent eight minute rinse resulted in 75% transfer of input oligonucleotides from one step to the next, while the less-stringent three minute rinse transferred 86% of input oligonucleotides from step to step. Additional experiments confirmed that photobleaching caused by repetitive imaging of the same input population had a negligible effect on the measured fluorescence intensity; protocols using less stringent hybridization conditions

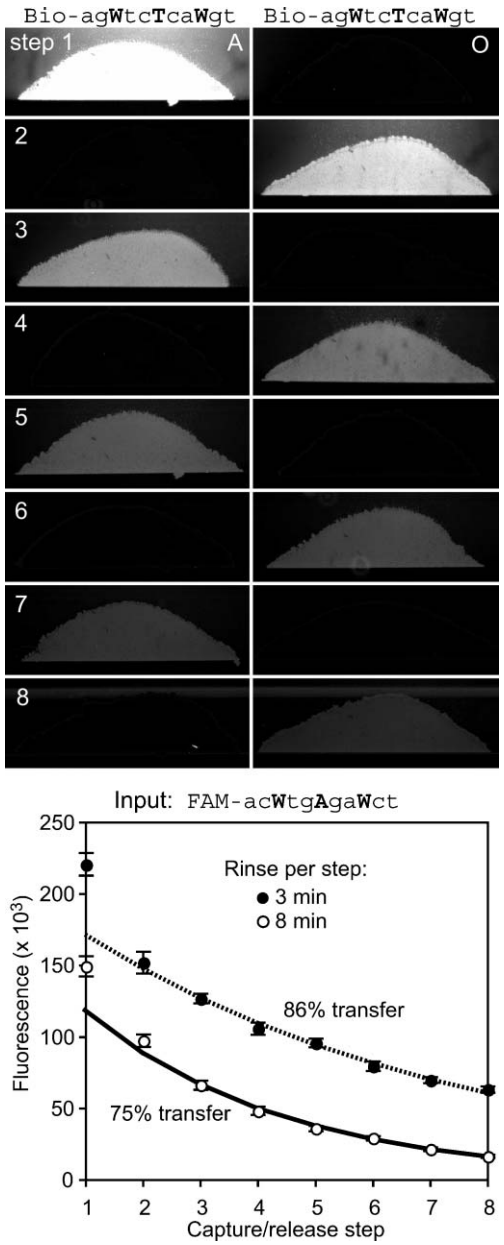

Fig. 4 Fluorescence images of the capture beads in both chambers at each step in the capture/release efficiency measurement, with 30 min capture and 8 min rinse after each capture/release step and a 3 s exposure. The back and forth pattern of fluorescence confirms the sequential transfer of perfectly-complementary input oligonucleotides between chambers A and O. In the accompanying plot of fluorescence counts from the capture chambers, using the more-stringent 8 min rinse after each capture step (open circles) results in a 75% step-to-step transfer efficiency (solid line), while a less-stringent 3 min rinse (closed circles) increases the transfer efficiency to 86% (dotted line).

increased transfer efficiencies to nearly 99% but were unsuitable for single-base mismatch detection.

For both rinse times, the amount of input DNA lost when transferring between steps 1 and 2 was larger than predicted by the calculated transfer efficiencies; a smaller loss was observed using the longer eight minute rinse time. This loss was attributed to excess nonspecific binding of input DNA to

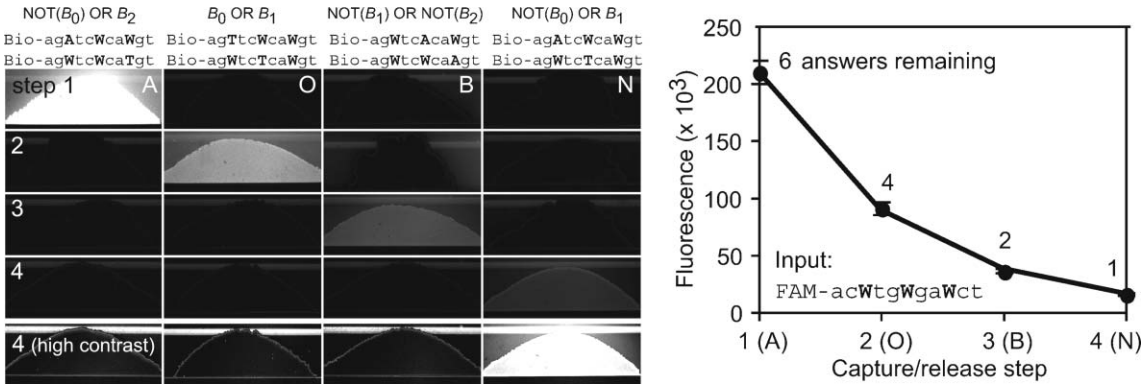

Fig. 5 Fluorescence images (3 s exposures) of beads in the four computation steps involved in the solution of the problem [NOT(B_0) OR B_2] AND [B_0 OR B_1] AND [NOT(B_1) OR NOT(B_2)] AND [NOT(B_0) OR B_1]. The decrease in fluorescence from step 1 to step 4 corresponds to the elimination of the seven different incorrect answers to the problem. The enhanced contrast images of step 4 show that the input oligonucleotides representing the correct answer to the problem have been captured uniquely in chamber N. In the plot of fluorescence intensity in the computing steps, the solid line traces a calculated elimination of half of the fluorescence intensity per step (as expected from the computation) plus an additional 8% loss (92% step-to-step transfer efficiency), which matches the observed data points accurately.

the beads that was more significant at the high input oligonucleotide concentrations present in the first capture step (30 μM) and less significant at the lower input oligonucleotide concentrations in the second (3.2 μM) and subsequent steps. For this reason, subsequent experiments were performed using an eight minute rinse (1.1% error) in the first capture/rinse/release step and a three minute rinse (7.6% error) in subsequent steps.

Satisfiability computation

In the satisfiability computation, 170 pmol of the input population FAM-acWtgWgaWct was loaded into the 5.8 μL loop volume and subjected to four serial capture/rinse/release steps representing the four clauses in the satisfiability problem. Fig. 5 presents fluorescence images of beads in the four computational chambers A, O, B, and N, at each of the four computation steps. The immobilized DNA contents and the computational role of each chamber are also indicated above each column. The loss of fluorescence observed as the initial 18 pmol of input oligonucleotides were transferred from A to O to B to N (30 min and ~22 passes through the bead suspensions per transfer) corresponds to the elimination of ~16 pmol of seven oligonucleotides encoding incorrect answers to the problem. Fluorescence counts decreased at a rate of 50% per step combined with a 92% transfer efficiency. In step 1, the input oligonucleotides FAM-acAtgTgaTct and FAM-acAtgAgaTct were captured by members of *both* Bio-agAtcWcaWgt and Bio-agWtcWcaTgt in chamber A. This increased the measured fluorescence in step 1 but had no effect on the outcome of the computation because FAM-acAtgTgaTct and FAM-acAtgAgaTct were eliminated completely in steps 2 and 3, respectively.

Three additional capture/release steps were then used to read out the identity (A or T) of each polymorphic base and the corresponding value (TRUE or FALSE) of each bit in the oligonucleotides captured in chamber N. The oligonucleotides were released and transferred to the first readout step by heating chamber N while pumping the oligonucleotides from N through chambers C and D simultaneously. Immobilized capture oligonucleotides in chambers C and D differed only at a single polymorphic base (A or T) at bit B_0, and the identity of the complementary base in the remaining input oligonucleotides (T or A) determined which one of the two chambers captured the oligonucleotides. This process was then repeated twice for the two remaining bits, using chambers L and M to read out the value of B_1 and E and F to read out B_2. Fig. 6 presents fluorescence images of the beads in the three readout steps (45 min each with no rinsing, 15 passes through each chamber). The higher fluorescence of Bio-agAtcWcaWgt

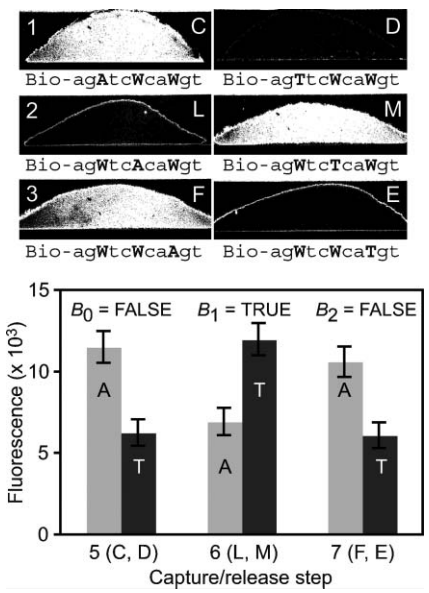

Fig. 6 Fluorescence images (3 s exposures) of beads in the three pairs of readout steps, with 45 min capture and no rinse for each step. In the analysis of the readout steps, the greater fluorescence intensities in chambers C (Bio-agAtcWcaWgt), M (Bio-agWtcTcaWgt), and F (Bio-agWtcWcaAgt) indicate that the remaining input oligonucleotides are predominantly FAM-acTtgAgaTct. The corresponding values of bits B_0 (FALSE), B_1 (TRUE), and B_2 (FALSE) encode the single correct answer to the problem. Bead fluorescence ratios are 1.8 for step 1 and 1.7 for steps 2 and 3.

This journal is © The Royal Society of Chemistry 2005

compared to Bio-agTtcWcaWgt (ratio = 1.8), Bio-agWtcTcaWgt compared to Bio-agWtcAcaWgt (1.7), and Bio-agWtcWcaAgt compared to Bio-agWtcWcaTgt (1.7) indicate that the remaining input DNA was predominantly FAM-acTtgAgaTct, and the corresponding bit values B_0 = FALSE, B_1 = TRUE, and B_2 = FALSE are the correct solution to the problem.

Discussion

The microfluidic processor presented here enables the fluidic manipulations necessary to utilize single nucleotide polymorphisms in DNA computing. Integrated monolithic membrane valves and pumps efficiently route a μL-scale loop of input oligonucleotide solution selectively between capture chambers. While existing DNA computers typically utilize single-passes of input oligonucleotides through a capture medium,[9,17] our microfluidic processor continuously recirculates the input oligonucleotide solution through the capture bead suspension at a rate of nearly one cycle per minute. The resulting improvement in hybridization kinetics makes possible the use of SNPs to represent binary bits in a hybridization-based DNA computation. This novel format requires only 1/8 of the capture time used in a current state-of-the-art computation employing constant 15-base capture sequences to represent each bit.[17] The use of SNPs to encode bits vastly simplifies the preparation of the DNA used in our computation, with a single synthesis run generating all possible answers to the problem. In our SNP computer, single base mismatches are identified with a 1.1% error, and the step-to-step transfer efficiency of 92% during the computation exceeds the 87% efficiency observed in previous computations.[17]

The most significant contribution to error proved to be nonspecific interactions between input DNA and beads early in the computation, which occur when the overall concentration of input DNA is highest. Increasing the rinse time from three to eight minutes for the first computation step reduced the effect of this error. We also found that the additional chambers in the fluid loop during the readout steps decreased the number of cycles of the fluid through each bead suspension from 22 to 15 passes and reduced bit fidelity; increasing the interrogation capture/release time further should compensate for the reduced number of cycles and improve upon the current mean ratio of 1.8 in Fig. 6. Finally, the use of fewer beads in the readout steps would further increase the fluorescence signal intensity, the sensitivity of the device, and the number of possible processor cycles.

A potential source of error as more complex problems are solved originates from the use of SNPs to represent binary bits. While the use of single nucleotide polymorphism ''wobbles'' to encode bits simplifies the task of preparing the input population, the method relies upon the destabilization caused by single-base mismatches for discriminating right answers from wrong ones. Chemical[26] or enzymatic[27] mismatch cleavage agents included in the rinse buffer could be used to nick imperfectly-matched input DNA for more effective elimination during rinsing. Also, since the outcome of the computation depends only upon detecting an *excess* of one base at each polymorphic locus, a technique like polymorphism ratio sequencing[28] could be used to detect as little as a 5% excess of one base at each polymorphic site.

The sensitivity of the microfluidic processor to single base mismatches also makes the device well-suited for the analysis of SNPs in biological assays. Assessing risk factors often requires not only the genotype of an individual but also the haplotype.[29] By modeling the haplotyping assay after the computation performed here and using genomic DNA fragments as the input information, it should be possible to obtain correlated SNP information using our microfluidic processor. While the SNPs detected here are separated by only a few bases, the single-base mismatch sensitivity of our device does not rely upon this proximity. Rather, 10- to 15-base capture sequences complementary to distinct and distant polymorphism-containing regions could be used to capture and route predetermined alleles; haplotype information would be revealed by sorting SNP populations through a series of steps similar to the AND and OR operations demonstrated here.

What are the ultimate computational capabilities of our microfluidic processor? Single nucleotide mismatches that reduce the duplex T_m by as little as 4 °C can be detected by hybridization.[30] Using the same experimental conditions as in this work, a nearest-neighbor hybridization thermodynamics model[25] predicts that an *8-bit, 10-clause* (10 step) satisfiability problem could be solved using the 10-base input population 5′-FAM-gW_8g-3′ with >4 °C difference between the least-stable perfectly-matched duplex and the most-stable single-mismatch duplex. Using 18 pmol of input DNA and a 92% step-to-step transfer efficiency as demonstrated here, 31 fmol of the single correct answer would be found at the end of the computation. In a device volume of 5.8 μL, the answer would be present at a concentration of 5.3 nM—an order of magnitude above the limit of detection of the fluorescence microscope used in this study. Such a result would be a significant advance over previous molecular computations employing eight polymorphic bases to solve 4-bit, 5-clause satisfiability problems.[31,32]

Solving problems larger than 8 bits and 10 clauses will require a larger-scale processor, a more extensible encoding scheme, and a more sensitive detection method. We expect that further miniaturization of the processor features (capture chambers, valves, *etc.*) will be possible and will result in improved capture efficiency, decreased reagent consumption, and reduced computation time. Additionally, since the current 16-chamber device utilizes only half of a 10 cm glass wafer, a processor fabricated on the full wafer could easily be extended to 32 capture/release chambers and used to solve 32-clause problems. A 32-chamber device would still require only two external magnet/heater assemblies, one on each side of the device. The most complex DNA computation completed to date, a 24-clause satisfiability problem, used long (300 base) input DNA containing constant capture sequences of 15 bases to represent each of 20 binary bits.[17] Larger computations can be performed using constant capture sequences because different 15-base sequences can be distinguished more easily than single-base mismatches. We anticipate that the improved capture and transfer kinetics that make single-base mismatch detection possible in our device will also improve the efficiency of multi-base capture. Using a 25-chamber device and 15-base

sequences to represent bits, a state-of-the-art 20-bit, 24-clause (24 step) satisfiability problem solved with 18 pmol input DNA and 92% transfer efficiency would result in 10^6 molecules encoding the single correct answer at the end of the computation—a population easily detectible by PCR and possibly also detectible by direct fluorescence means. We expect that the improved capture kinetics, step-to-step transfer efficiency and automation of our microfluidic processor will make it a valuable platform for many types of next-generation molecular computations.

Acknowledgements

Device fabrication was performed in the University of California, Berkeley Microfabrication Laboratory. We thank Robert Blazej for stimulating discussions. This research was supported by generous donations from Affymetrix to the Berkeley Center for Analytical Biotechnology.

References

1 L. M. Adleman, Molecular computation of solutions to combinatorial problems, *Science*, 1994, **266**, 1021–1024.
2 A. Gehani and J. Reif, Micro flow bio-molecular computation, *Biosystems*, 1999, **52**, 197–216.
3 T. Ohori, S. Shoji, K. Miura and A. Yotsumoto, Partly disposable three-way microvalve for a medical micro total analysis system (muTAS), *Sens. Actuators, A*, 1998, **64**, 57–62.
4 H. T. G. van Lintel, F. C. M. van de Pol and S. Bouwstra, A piezoelectric micropump based on micromachining of silicon, *Sens. Actuators*, 1988, **15**, 153–167.
5 P. A. Auroux, D. Iossifidis, D. R. Reyes and A. Manz, Micro total analysis systems. 2. Analytical standard operations and applications, *Anal. Chem.*, 2002, **74**, 2637–2652.
6 D. R. Reyes, D. Iossifidis, P. A. Auroux and A. Manz, Micro total analysis systems. 1. Introduction, theory, and technology, *Anal. Chem.*, 2002, **74**, 2623–2636.
7 S. Sjolander and C. Urbaniczky, Integrated fluid handling system for biomolecular interaction analysis, *Anal. Chem.*, 1991, **63**, 2338–2345.
8 X. Yang, C. Grosjean, Y. C. Tai and C. M. Ho, A MEMS thermopneumatic silicone rubber membrane valve, *Sens. Actuators, A*, 1998, **64**, 101–108.
9 J. S. McCaskill, Optically programming DNA computing in microflow reactors, *Biosystems*, 2001, **59**, 125–138.
10 D. van Noort and L. F. Landweber, Towards a re-programmable DNA computer, *Lect. Notes Comput. Sci.*, 2004, **2943**, 190–196.
11 H. Andersson, W. van der Wijngaart and G. Stemme, Micromachined filter-chamber array with passive valves for biochemical assays on beads, *Electrophoresis*, 2001, **22**, 249–257.
12 Z. H. Fan, S. Mangru, R. Granzow, P. Heaney, W. Ho, Q. P. Dong and R. Kumar, Dynamic DNA hybridization on a chip using paramagnetic beads, *Anal. Chem.*, 1999, **71**, 4851–4859.
13 J. W. Hong, V. Studer, G. Hang, W. F. Anderson and S. R. Quake, A nanoliter-scale nucleic acid processor with parallel architecture, *Nat. Biotechnol.*, 2004, **22**, 435–439.
14 A. B. Jemere, R. D. Oleschuk, F. Ouchen, F. Fajuyigbe and D. J. Harrison, An integrated solid-phase extraction system for sub-picomolar detection, *Electrophoresis*, 2002, **23**, 3537–3544.
15 G. H. Seong, W. Zhan and R. M. Crooks, Fabrication of microchambers defined by photopolymerized hydrogels and weirs within microfluidic systems: Application to DNA hybridization, *Anal. Chem.*, 2002, **74**, 3372–3377.
16 E. Verpoorte, Beads and chips: new recipes for analysis, *Lab Chip*, 2003, **3**, 60N–68N.
17 R. S. Braich, N. Chelyapov, C. Johnson, P. W. K. Rothemund and L. Adleman, Solution of a 20-variable 3-SAT problem on a DNA computer, *Science*, 2002, **296**, 499–502.
18 G. C. Kennedy, H. Matsuzaki, S. L. Dong, W. M. Liu, J. Huang, G. Y. Liu, X. Xu, M. Q. Cao, W. W. Chen, J. Zhang, W. W. Liu, G. Yang, X. J. Di, T. Ryder, Z. J. He, U. Surti, M. S. Phillips, M. T. Boyce-Jacino, S. P. A. Fodor and K. W. Jones, Large-scale genotyping of complex DNA, *Nat. Biotechnol.*, 2003, **21**, 1233–1237.
19 W. H. Grover, A. M. Skelley, C. N. Liu, E. T. Lagally and R. A. Mathies, Monolithic membrane valves and diaphragm pumps for practical large-scale integration into glass microfluidic devices, *Sens. Actuators, B*, 2003, **89**, 315–323.
20 B. M. Paegel, R. G. Blazej and R. A. Mathies, Microfluidic devices for DNA sequencing: Sample preparation and electrophoretic analysis, *Curr. Opin. Biotech.*, 2003, **14**, 42–50.
21 E. T. Lagally, J. R. Scherer, R. G. Blazej, N. M. Toriello, B. A. Diep, M. Ramchandani, G. F. Sensabaugh, L. W. Riley and R. A. Mathies, Integrated portable genetic analysis microsystem for pathogen/infectious disease detection, *Anal. Chem.*, 2004, **76**, 3162–3170.
22 A. M. Skelley, J. R. Scherer, A. D. Aubrey, W. H. Grover, R. H. C. Ivester, P. Ehrenfreund, F. J. Grunthaner, J. L. Bada and R. A. Mathies, Development and evaluation of a microdevice for amino acid biomarker detection and analysis on Mars, *Proc. Natl. Acad. Sci. USA*, 2005, **102**, 1041–1046.
23 P. C. Simpson, D. Roach, A. T. Woolley, T. Thorsen, R. Johnston, G. F. Sensabaugh and R. A. Mathies, High-throughput genetic analysis using microfabricated 96-sample capillary array electrophoresis microplates, *Proc. Natl. Acad. Sci. USA*, 1998, **95**, 2256–2261.
24 M. S. Livstone and L. F. Landweber, Mathematical considerations in the design of microreactor-based DNA computers, *Lect. Notes Comput. Sci.*, 2004, **2943**, 180–189.
25 N. Peyret, P. A. Seneviratne, H. T. Allawi and J. SantaLucia, Nearest-neighbor thermodynamics and NMR of DNA sequences with internal AA, CC, GG, and TT mismatches, *Biochemistry*, 1999, **38**, 3468–3477.
26 M. Grompe, D. M. Muzny and C. T. Caskey, Scanning detection of mutations in human ornithine transcarbamoylase by chemical mismatch cleavage, *Proc. Natl. Acad. Sci. USA*, 1989, **86**, 5888–5892.
27 P. C. Solaro, K. Birkenkamp, P. Pfeiffer and B. Kemper, Endonuclease-VII of phage-T4 triggers mismatch correction in vitro, *J. Mol. Biol.*, 1993, **230**, 868–877.
28 R. G. Blazej, B. M. Paegel and R. A. Mathies, Polymorphism ratio sequencing: A new approach for single nucleotide polymorphism discovery and genotyping, *Genome Res.*, 2003, **13**, 287–293.
29 N. Patil, A. J. Berno, D. A. Hinds, W. A. Barrett, J. M. Doshi, C. R. Hacker, C. R. Kautzer, D. H. Lee, C. Marjoribanks, D. P. McDonough, B. T. N. Nguyen, M. C. Norris, J. B. Sheehan, N. P. Shen, D. Stern, R. P. Stokowski, D. J. Thomas, M. O. Trulson, K. R. Vyas, K. A. Frazer, S. P. A. Fodor and D. R. Cox, Blocks of limited haplotype diversity revealed by high-resolution scanning of human chromosome 21, *Science*, 2001, **294**, 1719–1723.
30 M. Jobs, W. M. Howell, L. Stromqvist, T. Mayr and A. J. Brookes, DASH-2: Flexible, low-cost, and high-throughput SNP genotyping by dynamic allele-specific hybridization on membrane arrays, *Genome Res.*, 2003, **13**, 916–924.
31 L. M. Wang, J. G. Hall, M. C. Lu, Q. H. Liu and L. M. Smith, A DNA computing readout operation based on structure-specific cleavage, *Nat. Biotechnol.*, 2001, **19**, 1053–1059.
32 Q. H. Liu, L. M. Wang, A. G. Frutos, A. E. Condon, R. M. Corn and L. M. Smith, DNA computing on surfaces, *Nature*, 2000, **403**, 175–179.

 This journal is © The Royal Society of Chemistry 2005